



## INTERNATIONAL JOURNAL OF ENGINEERING SCIENCES & RESEARCH TECHNOLOGY

### Study on the Seizure Trends, Friction and Lubrication in a Total Hip Prosthesis with Self-Directed Balls

L. Capitanu <sup>\*1</sup>, V. Florescu <sup>2</sup>, C. Tiganesteanu <sup>1</sup>, D.C. Bursuc <sup>3</sup>

<sup>\*1</sup> Professor, Tribology Department, Institute of Solid Mechanics, 010141 - Bucharest, Romania

<sup>2</sup> Professor, Department of Mechanical Engineering, Institute of Civil Engineering, Bucharest, Romania

<sup>3</sup> Carol I Defence University, Bucharest, Romania

[lucian.capitanu@yahoo.com](mailto:lucian.capitanu@yahoo.com)

#### Abstract

Although Metal-On-Metal (MOM) Total Hip Prostheses (THP) with self directed balls have as their greatest advantage the replacement of the specific regular hip prostheses sliding movement between the femoral head and the acetabulum socket with the rolling movement between the balls, the socket and the femoral head, the lubrication side of the process is still not well known. Laboratory trials on the ball on the flat rig showed maximum values of the coefficient of friction under 0.05, and studies of lubrication with saline solution have indicated a lubrication schedule EHL, the minimum value for the thickness of the lubrication film ( $h_{min}$ ), measured through the contact resistance methodology, being 0.06  $\mu\text{m}$ , in the operation of these prostheses are obvious trends of seizure. The trials have been carried out in BSF (body simulated fluid) lubrication conditions, much closer to the real operating conditions up against the initial tests with distilled water. Seizure burdens to different loadings and contact surfaces roughness influence over the seizure burden have been determined. Even though the minimum value of the wear must be the same with the minimum value of the surfaces roughness, given the experimental conditions, it came out from the trials results on wear that the lowest level of wear is acquired at a certain value of roughness, not at the lowest level of roughness. There are obvious trends of seizure in the operation of these prostheses. However, preliminary studies on lubrication in MOM - THP also showed a clear seizure tendency. For the purposes of the present study we opted for changing the constructive version, adopting a modified motion Omnitrack solution, adapted for use in an artificial hip joint. After testing on an experimental device, the results were spectacular. The minimum friction coefficient value is 0.007, while the maximum value reaches 0.02.

**Keywords:** MOM THP, self directed balls, friction coefficient, friction evolution, lubrication

#### Introduction

All content Nowadays, the design solutions for THP (total hip prostheses) are diverse encompassing for improving the materials used for prostheses elements and reshaping geometrically and/or tribologically the load transfer path. In such context THP with rolling balls have been found as a possible viable alternative design to current industrial products, based on low friction of rolling contact, against sliding one (now used in most industrial designs). Different designs of THP with rolling bodies have been developed in order to improve the tribological performances of the artificial joint. We could mention here the design with ball train, proposed by Katsutoshi and Kiyoshi [1], the French "Supertête prostheses" [2], or the design with conical rolling elements proposed by Imperial College of Science, Technology and Medicine of London [3].

The French design, obtained by "The foundation for the future" in collaboration with The Ministry of Defence, Mission of Innovation, proposes the insertion of a frictional contact inside a bearing. The design suggested by Imperial College of Science, Technology and Medicine of London consists in a major modification of elements between the femoral part stem neck and the modular hip prosthesis by introducing a rolling bearing with conical femoral artificial head.

The bearing rotation axis corresponds with the axis of femoral stem neck, the rolling elements being guided by both the external surface of stem neck and the internal surface of the ball replacing the femoral head. But changing the contact mechanism from sliding to rolling in a hip prosthesis is not an easy task due to difficulties encountered in establishing the load transfer path, a critical

characteristic of tribological behavior of joint with large influence in functionality and durability of prosthesis active elements. Basically, the sliding contact between large surfaces of femoral head and acetabular cup was replaced by a multitude of rolling contacts with a different pattern of stress distribution influenced by rolling elements position at some instant during relative movement between femoral and acetabular parts. In the present paper, the authors focus on the seizure trends, friction and lubrication on the original design proposed by them in Ref. [4], i.e., a MOM-THP with self-directed rolling balls. A characteristic of this design solution is the fact that the artificial joint will work similar to a spherical bearing, having what is called a “compensation space”, i.e., enough free space between the femoral and acetabular parts of the prosthesis to allow the movement of the balls. Previous research studies performed by the authors focused on the determination of the initial position of rolling balls due to geometrical restraints of the assembly and on the estimation of the overall friction coefficients in dry and lubricated motion [5]. The geometrical studies [6, 7] have shown that generally the balls are located non-symmetrically and that the configuration for a given space and a given number of balls is not unique. Tribological studies performed by the authors of Refs. [4, 6, 7] have shown very low values of overall friction coefficients (0.12 to 0.2 for dry joint and 0.006-0.009 in the presence of lubricants), leading to an enhanced functionality of the prosthesis itself.

Lessons learned from previous attempts (structural overall analysis performed in Ref. [8]) lead to decoupling the statics and dynamics of the joint (FE analyses) from the tribological behavior (separate analytical evaluation) in order to save computational effort and assuming simplifications. After performing the geometrical assessment, based on the methodology presented in Ref. [4], it results that the maximum number of balls needed for the spherical joint is 199, distributed on 12 consecutive rows [9].

In 1970, in a reference paper, D. Dowson [10] was the first to appreciate the lubrication of MOM total hip prosthesis is elastohydrodynamic (EHL). This approach is considered also today. Thus, Leiming Gao, Fengcai Wang, Peiran Yang and Zhongmin Jin [11] presented a simulation of elastohydrodynamic (EHL) lubrication of a metal-on-metal (MOM) total hip implant, considering both equilibrium state and the physiological load transient state, as the movement during the gait cycle in all three directions. Numerical calculations presented, based on simulations are able to easily and accurately

reproduce loading and 3D movement. Because lubrication is closely related to the friction and wear of MOM hip bearings, lubrication analysis provides a better understanding of the high difference in the wear test results. Leiming Gao reported on the effect of surface texturing on the elastohydrodynamic lubrication analysis of metal-on-metal hip implants, that shows an advanced numerical model to simulate the mixed EHL problem of a MOM hip prosthesis with surface textured with pits. The results showed that this surface texture can have a beneficial effect on the reduction potential of the asperities contact ratio and the improvement of lubrication performances in MOM hip replacements.

Qingen Meng, Leiming Gao, Feng Liu, Peiran Yang, John Fisher and Zhongmin Jin [12] reported that the diameter and diameter tolerance of the bearing surfaces of metal-metal hip implants and the structural supports are key factors to reduce dry contact pressures and improve the performance of hydrodynamic lubrication. On the other hand, the application of aspheric bearing surfaces can also significantly affect both contact mechanics and lubrication performance by changing the radius of curvature of a bearing surface and consequent improvement of conformity between head and cup.

Pourzal R. et al [13] published a paper on micro-structural alterations in different areas of the articulated surfaces of metal on metal system, wherein show that nanoscale wear particles produced represent a limitation due to the harm of the human body. Y. Yana, A. Neville, D. Dowson, S. Williams and J. Fisher [14] published a paper related to the effect of metallic nanoparticles on biotribocorrosion behavior of metal on metal hip prostheses, which focuses on the particles in the third body and their effect on tribology and corrosion processes of bearing surfaces. A hip motion simulator integrated with an electrochemical cell was used to study the biotribocorrosion system. C.X. Li, A. Hussain and A. Kamali [15] presented some considerations on non-bearing surfaces conditions and their potential effect on the results of simulation tests for hip wear. It is shown that the potential mass loss on the non-bearing surfaces (specimens) and its contribution to the total results of gravimetric measurements are rarely mentioned in the specialized literature.

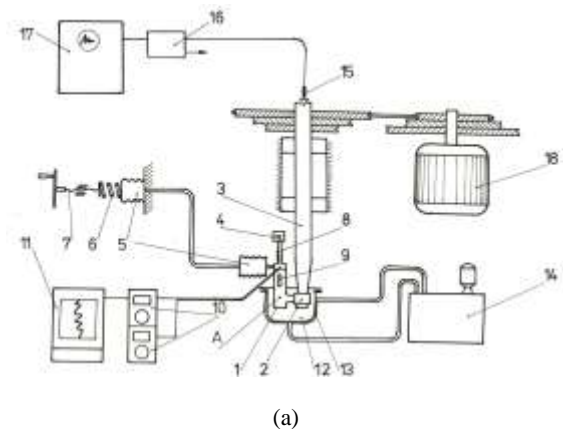
Osterle W. et al [15] published a paper about the wear resistance potential of the layers deposited on Ti-6Al-4V alloy for artificial hip joint bearing surfaces, where reports on the tribological tests (sphere/ plane) that were made by them, in order to identify a suitable coating for articulated surfaces of artificial hip joints whose acetabular cups and femoral stems are made of Ti6Al4V alloy. This alloy

is highly appreciated for its low weight, good compatibility and elastic properties similar to those of natural bone. With all the studies and improvements presented, the wear continues to be presented in the latest generation of MOM-THP. Nowadays, the design solutions for THP are diverse encompassing for improving the materials used for prostheses elements and reshaping geometrically and/or tribologically the load transfer path. In such context THP with rolling balls have been found as a possible viable alternative design to current industrial products, based on low friction of rolling contact, against sliding one (now used in most industrial designs).

The aim of this work was to determine how does occur the friction and lubrication, and also cause of the appearance of seizure trends. Stresses and deformations analysis for hip joint prostheses with rolling bodies in self-directed motion and preliminary study on the lubrication has been presented elsewhere [16].

**Materials and methods**

Preliminary study on the lubrication of a MOM-THP with self-directed balls revealed a certain seizure in some strain conditions. Laboratory trials for balls/plane Hertzian contacts have been restarted in order to determine seizure behaviour depending on the roughness of the flat area. The trials have been carried out in BSF (body simulated fluid) lubrication conditions, much closer to the real operating conditions up against the initial tests with distilled water. Seizure burdens to different loadings and contact surfaces roughness influence over the seizure burden have been determined. Even though the minimum value of the wear must be the same with the minimum value of the surfaces roughness, given the experimental conditions, it came out from the trials results on wear that the lowest level of wear is acquired at a certain value of roughness, not at the lowest level of roughness [16]. For the tests, we used the test rig presented in Fig. 1(a). In this test rig, the friction pair is formed from a bush with spherical profile and a flat disk shaped with a diameter of 18 mm and a thickness of 5 mm, Fig.1 (b). The sphere's radius is  $r = 11.5$  mm .



(a)  
 (b)  
**Figure 1. Experimental testing rig (a) and used friction samples (b).**

In the static contact, compression stresses in contact spot,  $p_{max}$  and  $p_{med}$  (maximum pressure and mean pressure) are

$$p_{max}^3 = 1.5PE^2 / \pi r^2 (1 - \mu^2) \tag{1}$$

$$p_{med} = \frac{P}{\pi a^2} \tag{2}$$

and the radius of the contact surface,  $a$ , is

$$a^3 = 1.5(1 - \mu^2)P \frac{r}{E} \tag{3}$$

where  $P$  is the load,  $a$ —radius of the contact surface, and  $r$ —radius of the sphere.

In the friction couple components (Fig. 9) are made f steel, the quantities of Eqs. (5) - (7) become

$$P_{\max} \approx 5800^3 \sqrt{P} \quad (4)$$

$$P_{\text{med}} \approx 1700^3 \sqrt{P} \quad (5)$$

$$a \approx 0.09^3 \sqrt{P} \quad (6)$$

Attention was paid to processing of working surfaces of couples. Surface state defined by topography, microstructure of surface layer and oxidation state has a major influence on the wear process. Experimental determinations were made on these test conditions:

- Load: variable between  $P = 20 \div 30$  N for determining of seizure limit. A load of 50 N was used for wear tests;

- Attention was paid to processing of working surfaces of couples. Surface state defined by topography, microstructure of surface layer and oxidation state has a major influence on the wear process. Experimental determinations were made on these test conditions:

- Load: variable between  $P = 20 \div 30$  N for determining of seizure limit. A load of 50 N was used for wear tests;

$$\frac{h_0}{r} = 0.84 \left( \frac{\alpha u \mu_0}{r} \right)^{0.741} \left( \frac{Er^2}{P} \right)^{0.074} \quad (7)$$

where  $h_0$  - minimum thickness of lubricant film;  $r$  - radius of the sphere;  $\alpha$  - pressure coefficient of viscosity;  $u$  - sum velocity;  $\mu_0$  - dynamic viscosity at atmospheric pressure;  $E$  - reduced elasticity modulus;  $P$  - load.

Spatial form of lubricant film in the loaded area results from Figs. 2, (a) and (b), which represents two sections lubricant film, longitudinal and cross sections (in relation to the movement) by the symmetry axes. Curves were obtained experimentally, under close conditions to those used by Ku [9].

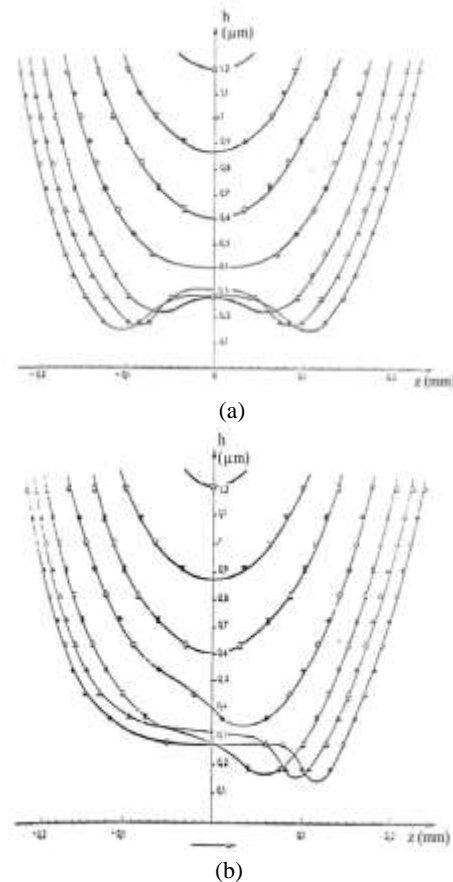


Figure 2. Variation of lubricant thickness in the  $x = 0$  plane (a) and variation of lubricant thickness in the  $z = 0$  plane, function of load (b), function of load, at speed  $u = 8$  cm/s, (a) and  $\blacksquare$  0.7 N;  $\blacktriangledown$  1.1 N;  $\square$  1.5 N;  $\diamond$  3 N;  $\blacksquare$  4.6 N;  $\blacktriangle$  7.8 N;  $\circ$  10.8 N.

Are noticed significantly higher values for minimum thickness  $h_0$ , even at speed  $u = 23$  cm/s. To watch in good conditions the wear of fixed surface, function of couple roughness, the following solution was used: roughness of the couple was focused on one of surfaces, in particular on the mobile one. Fixed surface had always the minimum roughness achievable, meaning about  $Ra \approx 0.015 \mu\text{m}$ . Under these conditions, and at a load  $P = 50$  N, speed  $u = 1.74$  m/s and volume temperature of the lubricant  $\theta = 50$  °C, it was determined the evolution of the surface wear based on time, for the following Under these conditions and at a load  $P = 50$  N, speed  $u = 1.74$  m/s and volume temperature of the lubricant  $\theta = 50$  °C, it was determined the evolution of the surface wear based on time, for the following roughness of the



mobile surface:  $Ra = 0.015 \mu\text{m}$ ;  $Ra = 0.045 \mu\text{m}$ ;  $Ra = 0.075 \mu\text{m}$ ;  $Ra = 0.19 \mu\text{m}$ .

For the study of fluid flow within the joint, three variants of calculation were considered, with several cases each.

1. Variant I studies the flow for a ball located between the cup and head of the joint, with consideration of undeformed geometry of surfaces in contact. The ball is tangent to spherical surfaces of the head and the cup.

2. Variant II analyzes the flow for a ball in the contact area with the head, considering the strain of the two surfaces, due to an interaction force between the ball and the head of 30 N. It is considered that although deformed, the ball is not in contact with the head, between them being a gap of 0.01 mm. The assumptions adopted are: geometries bide spherical except the contact area that is considered as a flat surface normal to the centers line (like a bevel).

3. Variant III analyzes the flow into the entire joint, considering some undistorted geometries. Small balls with radius lower with 0.01 mm were considered due to the FEM meshes difficulties.

In all cases presented above the wall of the cup is stationary, the wall of the femoral head is rotating and balls walls are also rotating around their centers in the directions specified in each computing case. The lubricant fluid, synthetic, SBF (Simulated Body Fluid) with density 1183 kg/m<sup>3</sup> and viscosity 0.84 Pa s (HyClone, SH30212.03) is considered incompressible. Computational Fluid Dynamics (CFD) is becoming more popular day by day, while on the other hand, the advanced technologies with huge memory and powerful processors at very low prices, which are able to solve large bi or tri dimensional numerical problems only in a few days. In another train of thoughts, commercial packages for CFD, such as FLUENT, make efficient numerical simulations easier than ever.

We considered that the flow is turbulent, turbulence model being the standard Spalart-Allmaras (SA) with an equation [17]. The linear model used by the Boussinesq hypothesis is:

$$\tau_{ij} = 2\mu_t \left( S_{ij} - \frac{1}{3} \cdot \frac{\partial u_h}{\partial x_h} \delta_{ij} \right) - \frac{2}{3\rho k \delta_y} \quad (8)$$

where the last term is generally ignored for Spalart-Allmaras, because  $k$  is not easily available (the term is sometimes ignored for unisupersonic flows of speeds for other models).

To study the flow for a ball located between the cup and head of the joint, by considering the undeformed geometry of surfaces in contact, was represented in Fig. 3(a) omitting domain, a fluid cell considering the ball walls, the femoral head (spherical surface with smaller radius) and the acetabular cup (spherical surface with larger radius), represented in black.

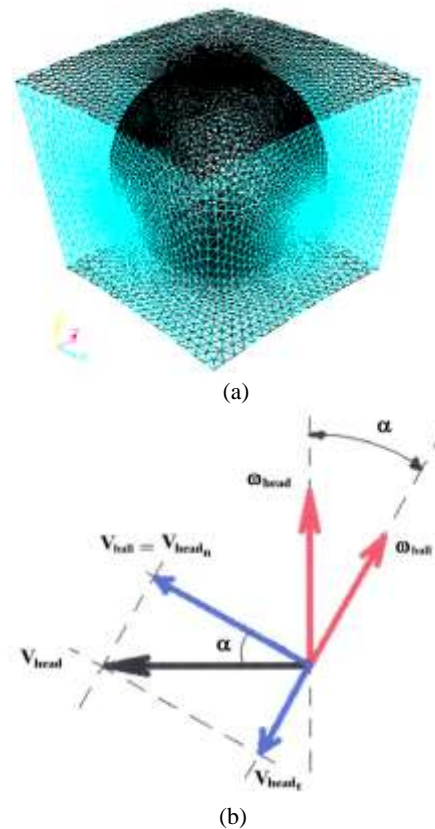
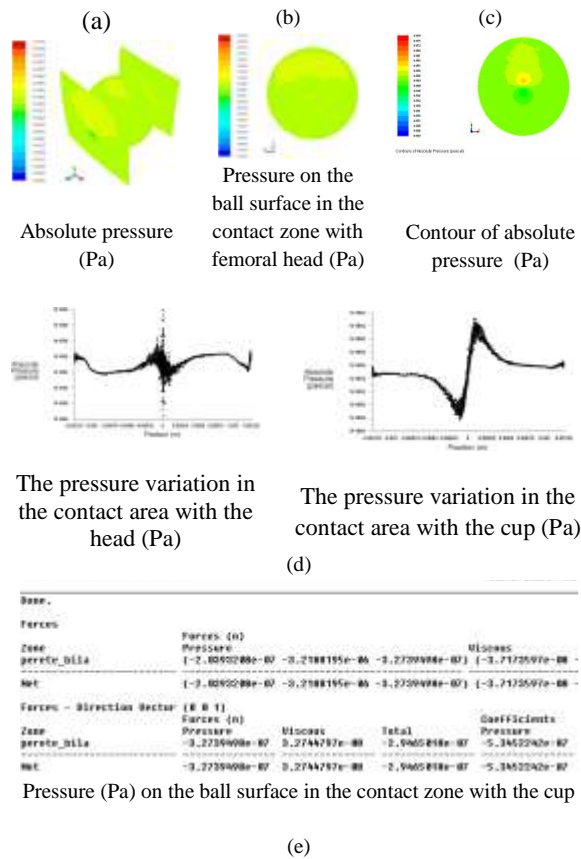


Figure 3. The lattice with tetrahedral elements (a) and (b) peripheral linear speeds in the contact geometric point and angular speeds of the head and the ball

Six angular speeds of the head are considered: 0.5; 1; 1.5; 2; 2.5; 3 rad/s and six slope angles of the angular speed of the ball as against the head: 0°, 15°, 30°, 45°, 60° and 75°.

For example, Figure 4 shows (a) the absolute pressure (Pa), (b) the pressure on the surface in the contact area with femoral head (Pa) and (c) the

numerical values recorded, in the case of a lubricant (BSF) pressure of 0.14 MPa.



**Figure 4. (a) The absolute pressure (Pa), (b) the pressure on the ball surface in the contact zone with femoral head (Pa), (c) contour of absolute pressure (Pa), at pressure of 0.14 MPa pressure, (d) the pressure variation in the contact area with the head and in the contact area with the cup (Pa) and (e) numeric values in the case of 0.14 MPa oil pressure.**

It is found, in all situations studied, a symmetrical distribution of pressure over the geometric focal point, both in the area of contact between the head and the ball, and in the contact zone between the cup and ball, leading to low values of the hydrodynamic forces. From the analysis of contact pressures in the contact areas, it is observed that the maximum pressures when the fluid is considered newtonian, with constant viscosity, are higher than the values determined for the fluid considered newtonian.

In terms of the minimum amount of pressure, it is remarked that the minimum values when the fluid is newtonian are greater than those determined in the case of newtonian fluid.

From the analysis of the pressure in the contact areas can be observed that the maximum pressures when the fluid is newtonian considered, with a constant viscosity, are higher than the values determined for the fluid considered newtonian. In terms of the minimum amount of pressure, it is remarked that the minimum values when the fluid is newtonian are greater than those determined in the case of newtonian fluid. Observe the differences in pressure distribution of motion plane (yOz) in the two areas of contact. Thus, although both points are seen rolling without slipping, is a lower level of pressure in the contact area between the head and the ball (where the centers of the spheres is apart of the tangent plane) relative to the area of contact between the ball and the cup (where the centers of the spheres are of the same side of the tangent plane).

The minimum thickness of the lubricating film in case the pressure of 0.14 MPa was found as 0.045 μm (Fig. 4), smaller than in case of using the method of contact resistance in the lab tests ball on flat (0.06 μm),

Total hip prosthesis with the balls in self-directed movement may be a viable solution for the durability increasing of total hip replacements. The results obtained in experimental conditions of this study, showed that in the case of consideration of the lubricant used (Body Fluid Serum - BSF) as a newtonian fluid were obtained pressures in contact area of the acetabular cup / ball / femoral head, more larger than for his consideration as a non-newtonian fluid.

Lubricant film exist, but is torn because of the oscillating movement (30°) in which the prosthesis it was tested, when ends of trace speed reaches the zero value. In these positions, contact pressure change their meaning - Fig. 4(e), causing seizure tendencies.

The maximum contact pressure with the lubricant used, was higher on the femoral head (0.142500 - 0.112100 MPa) and less on the acetabular cup (0.141848 - 0.111449 MPa), probably due to the difference of distance from the center of the femoral head. This study has some limitations. The main limitation is the condition of movement used. Testing is required in terms of continuous motion, which virtually eliminate zero speed points, from switching the direction of movement.

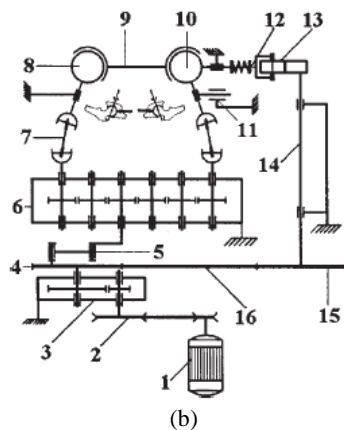
Another limitation is the duration of the calculation in Fluent, which imposed taking into account to a limited number of balls, as well as to neglect some of the contacts between the balls. Also another limitation lies in the uncertainty of the rheological nature or non- rheological of lubricating

fluid. In the present research we used an experimental device with two total hip prostheses joints mounted in anatomical position, whose movement reproduces the flexion - extension movement of the of human hip joint [16]. The results are very promising.

The device presented in Fig. 5 has been designed for experimental tests. The main features of this device are: simultaneous/alternative measurements of of the friction coefficient; perfect timing in the kinematic and dynamic simulation of the hip joint; compliance with the angle formed by the load axis and the oscillation axis.



(a)



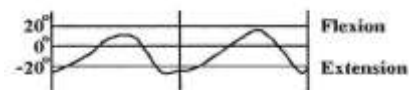
(b)

**Figure 5. Testing device (a) and kinematic diagram of testing device (b): 1 - electromotor; 2 - trapezoidal belts; 3 - recurrent reducing gear; 4 - wheel driving chain; 5 - gear box; 6 - gear reducer recurrent (periodic); 7 - universal joint; 8 and 10 - femoral heads; 9 - acetabular double piece; 11 - shaft; 12 - coupling with wedge and pull spline; 13 - cam; 14 - shaft; 15 - driven sprocket; 16 - Gall's chain.**

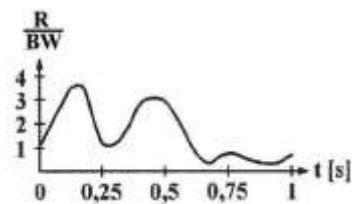
Figure 5 (b) shows the kinematic diagram of this device. The device was built in such a way that the acetabular double piece is supported by only the two femoral heads that oscillate in two directions,

similar to a hip. You can also see that the acetabular double piece moves at the same time as the femoral heads due to friction (Pos. 8 and 10).

The measured friction torque is a projection of the real torque, the latter resulting from the calculations. A cam - till - helicoidal compression spring (Fig. 5, pos. 12) accomplishes the specific load to the hip articulation. The cam (Fig. 5, pos. 13) was synthesized according to the loading diagram (Fig. 4b). The cam was rocked in the rotation of the chain (Fig. 5, pos 4, 15, 16) and a shaft (Fig.5, pos. 14). The flexion-extension movement was described by a quadrilateral gearing (Fig. 5, pos. 5), which has turned the chain wheel rotation (Figure 2, pos. 4) into an oscillation (Fig. 6)/



(a)



(b)

**Figure 6. (a) Variation of the flexion - extension over two gait cycles and (b) variation of the ratio  $R / BW$  during a normal gait cycle.**

This movement had a 1 Hz frequency (achieved by reducing the angular velocity generated by the electric motor, position 1, through trapezoidal belts transmission, position 2 and a repeating gear reducer, position 3). Oscillation has been transmitted to the femoral head by means of a chain with bolts, with the ratio of 1:1 (Fig. 2, item 5) and a cardanic universal coupling. For each gait cycle determinations of the friction coefficient were made for both the self directed balls joint (SDBJ) and for a type of Omnitrack® solutions movement, modified and adapted to the purpose (MOSMJ).

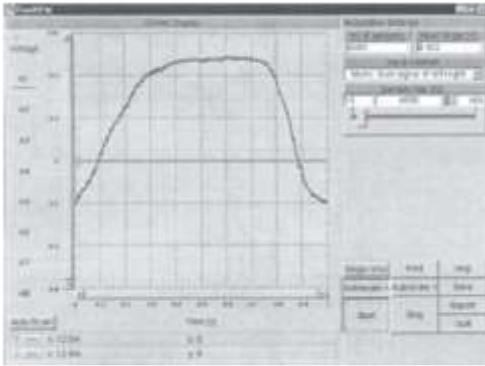


Figure 7. Variation of  $x$  displacement during a complete gait cycle.

### Results and discussion

The main purpose of this study was to determine the friction coefficient and to try to establish the optimum lubrication conditions.

We could express the experimentally determined dissipated power associated with a full gait cycle as:

$$P_{DE} = M_{fE} \cdot |\omega_{pa}| \quad (1)$$

where:

$P_{DE}$  is the experimentally determined dissipated power associated with a full gait cycle;  $M_{fE}$  is the experimental friction moment, and  $\omega_{pa}$  – the angular (variable) velocity of the acetabular component.

The angular velocity is implicitly taken as positive for the purposes of obtaining a positive dissipated power in the cycle.

The measured friction moment is:

$$M_{fm} = k \cdot x \cdot l \quad (2)$$

where:

$k$  – the spring's elasticity parameter ( $k = 14 \text{ N/mm}$ );  
 $x$  – the spring's deformation or the plate displacement;

$l$  – the length of the rigid plate ( $l = 63 \text{ mm}$ ).

The rigid plate displacement,  $x$ , has been experimentally determined as being the double of  $M_{fx}$  (figure 5). The angle of the resultant  $R$  and the flexion-extension axis is  $70^\circ$  while the experimentally determined friction moment,  $M_{fE}$ , is:

$$M_{fE} = \frac{1}{2 \cdot \cos 70^\circ} \cdot M_{fm} = \frac{k \cdot x \cdot l}{2 \cdot \cos 70^\circ} \quad (3)$$

The experimental dissipated power is the scalar product of the friction moment and the angular velocity of the double acetabular piece,  $\omega_{pc}$ :

$$P_{DE} = \overline{M}_{fE} \cdot \overline{\omega}_{pc} = M_{fE} \cdot |\omega_{pc}| \cdot \cos 70^\circ \quad (4)$$

$$P_{DE} = \frac{1}{2} \cdot k \cdot x \cdot l \cdot |\omega_{pc}|$$

The angular velocity of the acetabular piece is expressed in relation to the extremities of the rigid plate as  $v_f$ :

$$|\omega_{pc}| = \frac{v_l}{l} \cdot \frac{|\Delta x|}{\Delta t} \quad (5)$$

This leads us to express the dissipated power as:

$$P_{DE} = \frac{k \cdot x}{2} \cdot \frac{|\Delta x|}{\Delta t} \quad (6)$$

The experimental dissipated power must be equal to the theoretical power:

$$P_{DT} = P_{DE} \quad (7)$$

The above equality allows us to obtain the friction coefficient:

$$\mu = \frac{P_{DE}}{P_{fTE}} \quad (8)$$

where  $P_{fTE}$  is the theoretical power dissipated through friction. Therefore:

$$\frac{1}{\mu} = \frac{P_{fTE}}{P_{DE}} = \frac{1}{\mu_E} \quad (9)$$

where  $\mu_E$  is the elastic component of the friction coefficient.

Both the Total Hip Prostheses with Self Directed Ball Joint (SDBJ) – Fig. 7, as well as a new prostheses (MOSMJ) – Fig. 8, have been tested, the latter being based on a constructively modified Omnitrack™ [22] movement solution.



Figure 7. Acetabular cup - femoral head joint with balls in self directed movement (SDBJ).



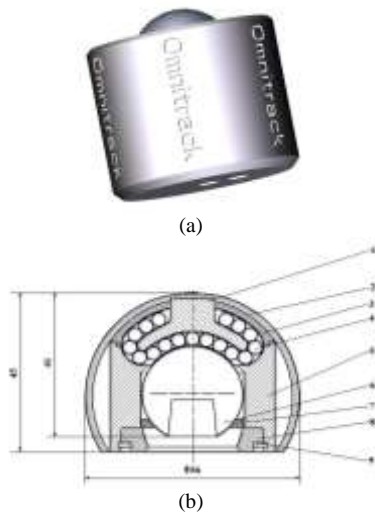


Figure 8. Stainless steel 316L Omnitrack joint (a) with low friction ( $\mu = 0.005$ ), maximum speed 2 m/s, temperature range - 30 °C to + 160 °C, high shock resistance and (b) new acetabular - femoral joint (MOSMJ) based on the modified Omnitrack movement solution : 1 - balls guide; 2 - outside casing; 3 - superior handle; 4 - ball; 5 - lower handle; 6 - femoral head; 7 - silicone rubber linings; 8 - lid; 9 – “Spiralax” ring.

We’ve named this new device a “femoral joint with self directed balls in Omnitrack® movement solution, modified (OSMJM)”.

The modified joint is a type 9030 [22], all of its components being manufactured out of medical grade SS316L stainless steel in order to provide very low friction ( $\mu = 0.005$ ). For a maximum 2 m/s velocity the joint can sustain a maximum 375 kg load and can optimally function between - 30 °C and + 160 °C. The joint is highly resistant to shocks.

In order to obtain the modified joint (Fig. 8a), the exterior component of the Omnitrack solution has been processed by turning so that it could fit into a medical grade 316L stainless steel casing and create the cocco – femoral prosthetic joint.

The Omnitrack™ movement solution (Fig. 8b) also had its functioning position changed by 180°. The ball guide, pos. 1 in Fig. 8(b), has been manufactured out of AmAlOx ceramic alumina in order to improve its seizure resistance. AmAlOx 87 alumina (Astro Met Aluminum Oxide) comes from Astro Met, Inc., Cincinnati, OH, USA. It’s a high purity 99.8% aluminum oxide (alumina) ceramic which has been originally developed for critical load bearing medical implants, and optimized for maximum wear and corrosion resistance.

A high density, diamond like hardness, fine grain structure and superior mechanical strength are its unique properties that make the AmAlOx alumina the appropriate material for demanding applications. The typical properties of AmAlOx 87 alumina include a bulk density of 3.97 g/cm<sup>3</sup>, flexural strength of 70

KPSI (482 MPa), Vickers Hardness of 2000 and a grain size of 2 microns. AmAlOx 87 alumina has an unusually small grain size for an alumina ceramic and this enables extremely tight tolerances and surface finishes of 2 microinches  $R_a$  to be achieved when the proper finishing techniques are being used.

**Results and discussion**

Figure 9 detail the real time variation of the friction coefficient in relation to the angular velocity and the load during a full 1 second gait cycle, for the SDBJ joint, on the testing device shown in Figure 1.

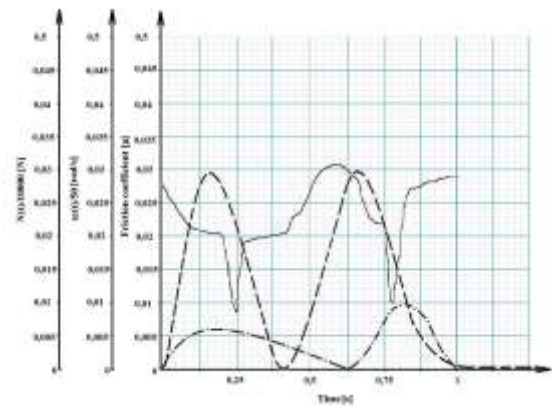


Figure 9. Comparison between friction coefficient and the angular velocity modulus, for the self directed balls acetabular - femoral joint (SDBJ) in Figure 7. It is worth noting that there is an inverse dependency between the friction coefficient and the load and a direct dependency with the angular velocity. —  $\mu (t)$ ; - - -  $N (t) / 10000 [N]$ ; · · · ·  $\omega (t) / 25 [rad /s]$

Figure 10 detail the real time variation of the friction coefficient in relation to the swame variables and in same conditions to the OSMJM femoral joint.

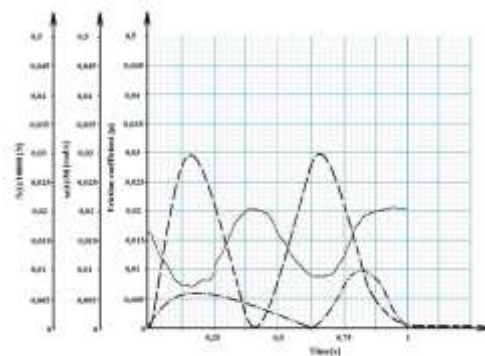


Figure 10. Comparison between friction coefficient and the angular velocity modulus, in the case of the acetabular - femoral joint with self directed balls in the modified Omnitrack® solution (OSMJM). It is worth noting that there is an inverse dependency between the friction coefficient and the load and a direct dependency with the angular velocity. —  $\mu (t)$ ; - - -  $N (t) / 10000 [N]$ ; · · · ·  $\omega (t) / 25 [rad /s]$ .

The maximum load used was 3000N for an angular velocity of 1 step / second. Comparing the two diagrams allows for a few observations.

The minimum values of the friction coefficient for the SDBJ and the OSMJM joints are 0.009 and 0.006 respectively. The maximum values of the friction coefficient for the SDBJ and the OSMJM joints are 0.031 and 0.02 respectively. The average values of the friction coefficient for the SDBJ and the OSMJM joints are therefore 0.022 and 0.016 respectively.

The average values of the friction coefficient for the SDBJ and the OSMJM joints are therefore 0.022 and 0.016 respectively. The sudden decreases in the friction coefficient values (the troughs) are due to the almost frictionless rolling of the balls on the femoral head. The two peaks are representative of the "heel strike" [21] phase in the gait cycle. Peaks occur when a greater number of balls become engaged in motion and slide on the femoral head.

Figs 9 and 10 shows a time comparison between the friction coefficient, the angular velocity modulus and the load, SDBJ and in the low friction Omnitrack joint, OSMJ.

The peculiar shape of the curve that plots the variation of the friction coefficient is due to the overlapping of the friction phenomena specific to the sliding and rolling movements, respectively.

It's a well known fact that the velocity and the load are the main factors that influence the friction coefficient values. Consequently, given the aforementioned experimental conditions, a periodical variation was expected and occurred in the recorded results, due to the rolling movement of the tested devices.

Studying the periodic nature of the friction coefficient values allows us to observe threefold increases in its values. We can explain this through the fact that the recorded coefficient values are the sum of the effects of the rolling motion and the sliding motion between the balls and the surfaces they come in contact with. What we are dealing with can therefore be called a global friction coefficient that sums up the effects of the different motions. The overlap of the effects is all the more visible in the SDBJ joint, where the sliding of the balls in the constructively designed free space that prevents the seizure of the ball array leads to slightly greater values for the global friction coefficient.

It's worth noting that the smallest values for the friction coefficient have been recorded in areas close to maximum loads, where a predominantly rolling motion takes place.

The recorded minimums for the two experimental devices also allow us to observe

different contributions of the sliding motions, although the values of the friction coefficient are very close.

In the OSMJM joint we also observe that, apparently, the angular velocity is not a main factor in the change in friction coefficient values, these being, in fact, inversely proportional to the load – we recorded minimum coefficient values for both minimum and maximum angular velocities.

The angular velocity becomes an important influencing factor for the SDBJ joint due to the overlap of the sliding and rolling motion effects. Thus, we recorded sudden decreases in the friction coefficient for maximum velocities and substantial loads – indicative of a predominantly rolling motion effect.

## Conclusion

Our research on the friction and lubrication in rolling motion hip prostheses allows us to conclude that:

- The friction coefficient is dramatically reduced compared to a classic sliding motion of the hip prostheses (Ti6Al4V/UHMWPE), whose minimum coefficient value is 0.05;
- the recorded values for the friction coefficient in the self-directed balls joint (SDBJ) range between 0.009 and 0.031, while those particular to the modified Omnitrack solution (OSMJM) range between 0.006 and 0.02;

- The average friction coefficient recorded value for the Omnitrack® modified solution (OSMJM) is 0.016;
- Maximum values correspond to the "heel strike" phase in the gait cycle;

- There's an overlap of friction phenomena specific to the rolling and sliding motions. This leads to peculiar changes in the friction coefficient values. We plan to investigate these variations in future research. - rolling motion THPs are a viable solution where sliding motion THPs are inappropriate due to the user's high body mass.

## Acknowledgements

The authors would like to thank the Romanian Academy for the material support it provided. They would also like to thank the Technical University "Gheorghe Asachi" of Iasi for the technical support that made this research possible.

## References

1. Xsu S., Ying Ch., Vasu D., Zhao F. "The nature of friction: A critical assessment. *Friction*. DOI 10.1007/s40544-013-0033
2. Dowson D. *Elastohydrodynamic lubrication. Interdisciplinary approach to the lubrication of*

- concentrated contacts” (Ed. P.P.KU) NASA SP – 237 (1970)
3. Gao L., Wang F., Yang P., Jin Z. Effect of 3D physiological loading and motion on elastohydrodynamic lubrication of metal-on-metal total hip replacements. *Medical Engineering & Physics* 31 (2009) 720-729.
  4. Páczelt I., Kucharski S., Mrózz. The experimental and numerical analysis of quasi-steady wear process for a sliding spherical indenter *Wear* 274-275 (2012) 127-148.
  5. Sharma S., Sangal S., Mondal K. On the optical microscopic method for the determination of ball-on-flat surface linearly reciprocating sliding wear volume. *Wear* 300 (2013) 82-89.
  6. Iliuc I. Wear and micropitting of steel ball sliding against TiN coated steel plate in dry and lubricated conditions. *Tribology International* 39 (2006) 607-615.
  7. Iliuc I., Jokl M. A comparative investigation of the sliding wear mechanism in lubricated steel-on-steel and diamond-on-steel friction pairs. *Wear* 176 (1994) 73-79.
  8. Brocket C., Williams S., Jin Z., Issac G., Fisher J. Friction of total hip replacement with different bearings and loading conditions. *Journal of Biomedical Materials Research Part B: Applied Biomaterials* DOI 10.1002/jbmb
  9. Munteanu F., Botez P. Variation of friction factor through the gait cycle in an UHMWPE-CoCrMo hip endoprosthesis. *Materiale plastice*, 45, 2, 2008, 131-136
  10. Javaherchi T. Review of Spalart -Allmaras turbulence model and its modifications. <http://www.ewp.rpi.edu/hartford/~ernesto/S2011>
  11. Spalart P.R., Allmaras S.R. A one equation turbulence model for aerodynamic flows. *Recherche Aerospaciale*, No. 1, 1994, pp. 5-21.
  12. Langley Research Center. Turbulence modelling resource. The Spalart-Allmaras turbulence model turbomodels larc nasa gov/spalart.html Langley Research Center. Turbulence modelling resource. The Spalart-Allmaras turbulence model turbomodels larc nasa gov/spalart.html
  13. Morales-Espejel G.E., Gabelli A. The behaviour of indentation marks in rolling-sliding elastohydrodynamically lubricated contacts. *Tribology Transactions*, 54: 589-606, 2011, DOI:10.1080/10402004.2011.582571
  14. Billis P.J., Racasam R., Underwood R.J., Cann P., Skinner J., Hart A.J., Jiang X., Blunt L. Volumetric wear assessment of retrieved metal-on-metal hip prostheses and the impact of measurement uncertainty. *Wear* 274-275 (2012) 212-219.
  15. Lugt P.M., Morales-Espejel G.E. A review of elasto – hydrodynamic lubrication theory *Tribology Transactions*, 54: 470-496, 2011, DOI:10.1080/10402004.2010.551804
  16. Meng Q., Gao L., Liu F., Yang P., Fisher J., Jin Z. Contact mechanics and elastohydrodynamic lubrication in a novel metal-on-metal hip implant with an aspherical bearing surface. *Journal of Biomechanics* 43 (2010) 849-857.
  17. Katsuoishi B., KIYOSHI S. United States Patent 5092898/Mar. 3, 1992, US005092898A KATSUOSHI B., Kiyoshi S. US Patent 5092898 / 03.03.1992.
  18. Iarovici A, Capitanu L., Florescu V., Baubec M. Hip Joint Prosthesis with Rolling Bodies. *Proceedings of the Romanian Academy – Series A: Mathematics and Physics, Technical Sciences, Information Science*, 1, 1-2, pp. 37-44, S. 2001.
  19. Capitanu L., Florescu V. New Concepts for Improved Durability in MOM Total Hip Endoprotheses. A review. *American Journal of Materials Science* Vol.2, No. 6, December 2012.
  20. Capitanu L., Badita L-L., Florescu V., Bursuc D-C. Preliminary Study on the Seizure Trend of a MOM-THP with Self-Directed Balls. *Journal of Mechanics Engineering and Automation* Volume 3, Number 9, September 2013.
  21. Vaughan C.L., Davis B.L. O’Connor J.C. *Dynamics of human gait. Second Edition.* Kiboho Publishers, Cape Town, Suth Africa.
  22. Omni - Directional movement Solution, www.Omnitrack™ Co UK